

10th CIRP Conference on Photonic Technologies [LANE 2018]

Why is in situ quality control of laser keyhole welding a real challenge?

T. Le-Quang^{a,*}, S.A. Shevchik^a, B. Meylan^a, F. Vakili-Farahani^a, M.P. Olbinado^b, A. Rack^b, K. Wasmer^a

^aSwiss Federal Laboratories for Materials Science and Technology (Empa), Laboratory for Advanced Materials Processing (LAMP), Switzerland

^bEuropean Synchrotron Radiation Facility, station ESRF-ID19, Grenoble, F-38043, France

* Corresponding author. Tel.: +41-58-765-6201 ; fax: +41-58-765-6990. E-mail address: quang.le@empa.ch

Abstract

In this work, we investigated keyhole welding including the pore dynamics (creation and collapse) of aluminium at the European Synchrotron Radiation Facility (ESRF, Grenoble, France). Optical back reflection and acoustic signals were simultaneously recorded during the welding process which was also visualized by high-speed X-ray imaging. This allows correlating the different momentary events with the signals recorded by the sensors. We demonstrate that keyhole welding is a highly dynamical and unstable process. In addition, to use either acoustic or optical sensors for pore detection, highly advance statistical methods such as machine learning are a requisite for signal processing.

© 2018 The Authors. Published by Elsevier Ltd. This is an open access article under the CC BY-NC-ND license

(<https://creativecommons.org/licenses/by-nc-nd/4.0/>)

Peer-review under responsibility of the Bayerisches Laserzentrum GmbH.

Keywords: Laser welding; in-situ monitoring; acoustic emission, X-ray imaging

1. Introduction

Since the invention of laser sources in the 1960s [1], this technology has been involved in a large number of industrial applications, e.g. in automotive, electronic and medical sectors. Among them, laser welding is one of the most common. Even though the process has been extensively studied, the mechanism responsible for defects formation in the weld joint, in particular porosity, has not been successfully established [2]. It is partially due to the complexity of the laser-material interaction and the short lifetimes of the events such as the opening and collapse of the keyhole in its unstable state [3]. Consequently, control of the weld quality, though desirable, is challenging. Most of the proposed solutions rely on high speed cameras or optical sensors [4–6]. These methods are limited to the surface of the process zone and the plume and, therefore, are not efficient in probing the keyhole and the formation of pores in depth.

In our work, we propose the use of acoustic emission (AE) sensors in combination with optical emission sensors. Compared to optical and visual methods, the acoustic sensor records the shockwave generated in the workpiece during the

process [7]. Thus, it is supposedly more sensitive to the behaviors of the process zone such as the fluctuation of the keyhole and the formation of pores. Another advantage of this technology is the affordable hardware required. Hence, it has been implemented in industrial operation for monitoring similar processes such as additive manufacturing and arc welding [8,9].

The final aim of our work is to develop an in situ and real-time quality control of the process. Consequently, the signals collected by the AE and optical sensors must be correlated with the momentary events (e.g. spattering, pore formation and keyhole fluctuation) taking place not only at the surface but also inside the process zone. This correlation encounters several difficulties. Firstly, it is often made post mortem via analysis of cross-sections and, thus, only for visual defects (pores, cracks) [8,10,11]. Secondly, the AE and optical signals are known to be very complex. This procedure is subjected to errors due to the high dynamic of the laser-material in conjunction with the random fluctuations in the signals. To overcome this difficulty and to visualize the weld process in real-time, several series of laser welding experiments were

made with a state-of-the-art high speed X-ray imaging at the European Synchrotron Radiation Facility (ESRF).

2. Experimental method

The laser welding experiments were made with a single mode fiber laser source StarFiber 150P (Fiber laser – StarFiber 150P/300P – long pulse fiber laser systems) with a 1070 nm wavelength. The laser system was capable of both continuous-wave (CW) and pulse operational modes but only the latter was employed in this work. The emitted Gaussian beam was transmitted through a 12 μm diameter single – mode optical fiber to a laser head. The laser beam was guided by the optical system within the laser head and then focused on the sample surface by a focusing lens with a focal length of 170 mm. The diameter of the laser spot at the focus was approximately 30 μm at $1/e^2$ of the beam's maximum intensity. This small diameter allowed not only keyhole formation at low laser power but also to use thin sample (2 mm thick) that is necessary to see through via X-ray imaging.

The laser head also contained an optical system for collecting the co-axial back-reflected and/or emitted radiation from the process zone as depicted in Fig. 1a. The collected light was directed towards the sensor module containing three optical sensors: Si, Ge and AlGaAs sensors operating within the ranges 450 – 850 nm, 1000 – 1200 nm and 1250 – 1700 nm, respectively. This module was described in more details in a previous work [10]. Signals from the optical sensors were recorded using an oscilloscope (Teledyne LeCroy, USA) with a sampling rate ranging from 0.05 to 10 MHz, depending on the welding length. Even though all three optical sensors were recorded simultaneously during the experiments, only the results with the Ge sensor are presented in this work as some optical losses occurred in the connection, reducing the signal from the other sensor to noise level. For sensing the acoustic shockwave created during welding, an acoustic piezoelectric sensor Pico (Physical Acoustics, USA) sensitive within the range of 500-1850 Hz was used. The AE sensor was attached to the sample holder with a rubber band. The AE signals were

digitized and stored by a data acquisition unit and software from Vallen (Vallen GmbH, Germany). The sampling rate of the AE signals was fixed at 10 MHz. The acquisition units were triggered by the laser. Preliminary tests showed that the delay between the signal acquisition and the laser emission was less than 25 μs .

The high-speed X-ray imaging was carried out at beamline ID19 of the ESRF using the synchrotron X-ray source in polychromatic mode: high photon flux that could be exploited for X-ray radiography up to millions frames per second (fps) rates [12]. X-ray phase contrast imaging by free-space propagation was utilized to enhance the contrast between material interfaces. An U-13 type undulator (single harmonic) at minimum gap of 11.1 mm was used. A diamond filter and an aluminium filter of 1.4 mm thickness each suppressed the lower photon energies. The pink beam mean energy was 26.3 keV. The radiography of the laser welding process was recorded by an indirect X-ray detector composed of a 250 μm -thick Ce-doped $\text{Lu}_3\text{Al}_5\text{O}_{12}$ scintillator (Crytur, Czech Republic), lens-coupled to a high-speed camera (pco.dimax; PCO AG, Germany) at a 90° angle using a mirror. The recording frame rate during the experiments was fixed at 28762 fps. The effective pixel size of the X-ray image detector was 11 μm . The diagram of the setup for laser welding experiments is presented in Fig. 1b.

In our experiments, aluminum was chosen for the weld samples due to its high X-ray transmissivity. The aluminum samples manufactured for welding had a dimension of 2x20x50 mm^3 . The samples were placed to have a thickness of 2 mm along the X-ray path, allowing a transmission rate of approximately 54%. The samples were firmly fixed in the aluminum sample holder which is placed on a XYZ table.

A total of 40 welding experiments were performed. The samples were either stationary (spot weld) or moved with a velocity of 1.5 mm/s (seam weld) in a direction perpendicular to both the laser and the X-ray beams. Laser powers up to 250 W and pulse durations between 10 and 15 ms were chosen as process parameters to provoke different weld regimes. The pulse repetition rate was fixed at 10 Hz

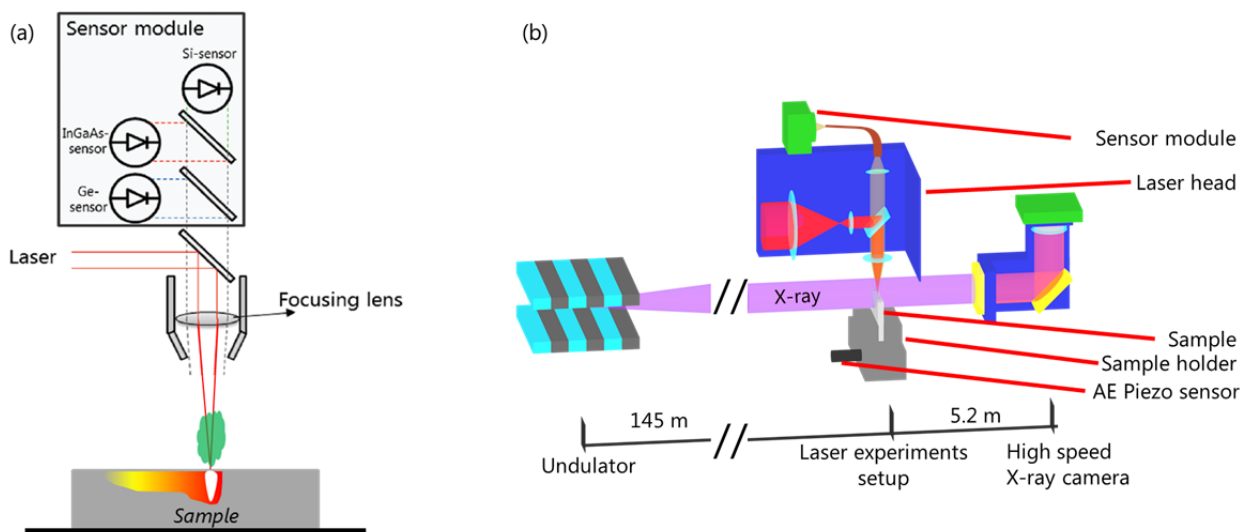


Fig. 1. (a) The diagram of the laser head including optical sensors, adapted from Vakili-Farahani et al. [10], and (b) The setup for the laser welding experiments.

(b) The setup for the laser welding experiments.

throughout the experiments.

3. Results and discussion

Figure 2 presents typical optical and AE signals recorded during the experiments. This particular experiment was performed with a single laser pulse at 250 W during 10 ms. The optical signal shows a significant increase in amplitude during the first 0.4 ms. It can be attributed to shallow melting of the sample's surface. No other remarkable feature is observed in this signal. In contrast, the surface melting stage cannot be clearly observed in the AE signal. However, several bursts with sub-millisecond durations can be clearly observed in this signal at around 2.5 ms, 3.4 ms, 6.0 ms, 8.3 ms and 9.3 ms, indicating intensive activities in the process zone. The observation shows that the optical and AE signals are sensitive to different physical events during laser welding. In addition, the complexity of the signals, especially the AE signal, suggests that the correlation between the signals and

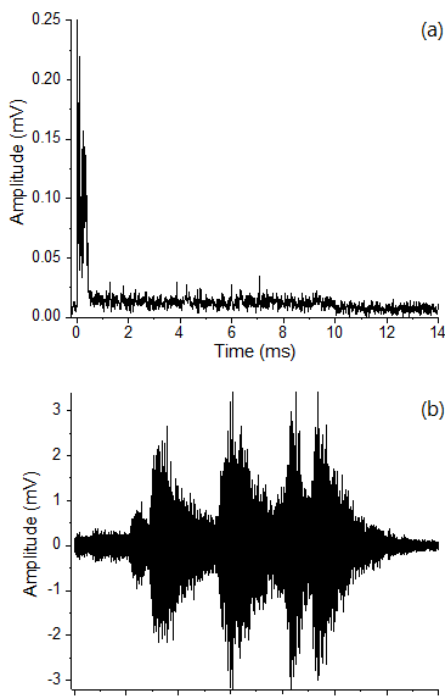


Fig. 2. Optical (a) and AE (b) signals recorded during a laser experiment with 250 W laser power and 10 ms pulse duration.

the process should be done via in situ imaging instead of post mortem analysis of the cross sections.

Figure 3 shows a sequence of X-ray images of the process zone during the experiment presented in Fig. 2 together with the record signals. The time t at which the image was taken is indicated in the images. t equals 0 at the beginning of the laser pulse. The components of the process zone could be distinguished based on their brightness. This depends mainly

on the density and, hence, the temperature of the matter. In particular, keyhole is characterized by the highest brightness as it contains mostly metallic vapor, while solid material showed the lowest brightness.

The X-ray images reveal a highly complex behavior of the process with numerous sub-millisecond events. In the first 0.38 ms of the laser pulse, only a small amount of molten material was observed (See Fig. 3 $t = 0.35$ ms). The shallow surface melting can be explained by the high reflectivity of aluminum at room temperature [13]. This leads to an inefficient coupling of the laser energy into the process zone. The melt pool expanded as the irradiation continued, increasing the laser absorption. The transition to keyhole took place when the pressure created by the evaporation of molten material was strong enough to push aside the melt pool forming a channel of metallic vapor. This formation causes an abrupt increase of laser absorption due to the multiple absorption of the laser by the keyhole walls. The improved energy deposition caused further expansion of the melt pool and the keyhole (0.38 – 0.63 ms). As the penetration depth of the keyhole increased, its instability increased as well. This behavior is often attributed to the surface tension of the molten material, which is responsible for the closing/collapse of the keyhole [3]. At sufficiently high penetration depth, the opening of the keyhole could not be permanently sustained and its partial collapses and openings could be observed (See Fig. 3 $t = 1.84$ – 9.67 ms). This rapid fluctuation could trap the metallic vapor in the keyhole channel, leading to pore formation mostly close to the tip of the keyhole (See Fig. 3 $t = 7.02$ ms) [14]. The created pores might either disappear by merging with the keyhole or moved away from it so that it remains present until the end of the process. Spattering, another undesirable event, also took place during the fluctuation of the keyhole (See Fig. 3 $t = 1.84$ ms). The X-ray results indicate that these behaviors of the keyhole took place simultaneously and on sub-millisecond time scales. At the end of the laser pulse, the keyhole collapsed abruptly while strongly fluctuating, resulting in trapping of the vapor. Consequently, a pore was formed, which remained in the sample afterwards.

The momentary events revealed by the X-ray images, especially during the unstable keyhole stage, have strong influence on the final quality of the weld. Nevertheless, they cannot be completely correlated to the recorded signals via human visual inspection. In particular, only the shallow surface melting can be visually recognized in the optical signal. On the other hand, the bursts observed in the AE signal within the range 2 – 10 ms can be attributed to the instability of the keyhole. In addition, part of the AE signal within the range 10.00 – 13.45 ms can be related to the resolidification of the melt pool. However, the transient events such as keyhole fluctuation, spattering and pore formation cannot be visually recognized in the signals.

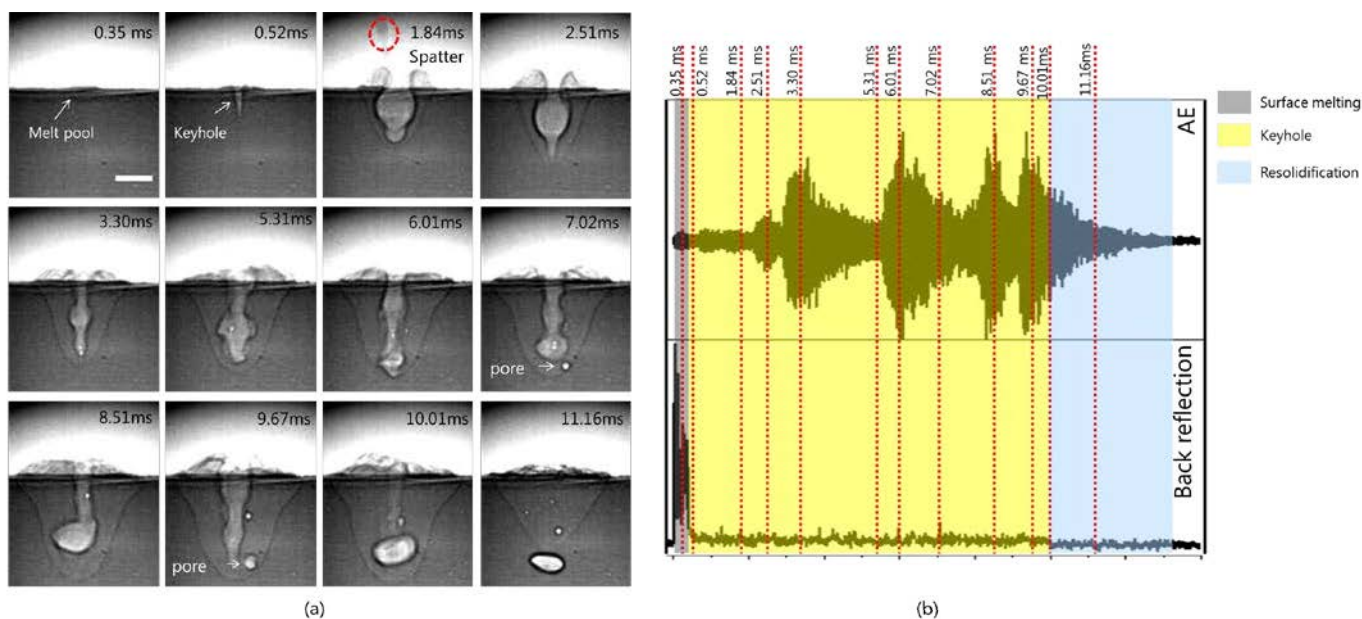


Fig. 3. X-ray images of the process zone (a) and the corresponding AE and optical signals (b) during an experiment at 250 W during 10 ms. The scale bar equals 300 μm . The times at which the images are indicated above the images and in the signals.

It can be concluded that human visual inspection of the signals is neither efficient nor reliable as the events took place simultaneously and at very short time spans (sub-millisecond). In order to distinguish the transient events, analysis of the signals in time-frequency domain using wavelet decomposition is known to be a much more efficient and reliable approach [10,15]. Furthermore, the application of machine learning techniques would be very useful in detecting the changes in the time-frequency components at the transition between different transient events [8,11]. Indeed, this approach was tested on the data from our present experiments and reported by Wasmer et al. [16]. Following events were defined based on the X-ray images: 1) *conduction welding*, 2) *stable keyhole*, 3) *unstable keyhole*, 4) *spatter*. The corresponding signals were analyzed by wavelet package transform (WPT) [17]. Event classification was done by gradient boost (GB) [18], an extension of a more general boosting technique [19], which is a branch of machine learning that employs a number of weak classifiers to build a strong one [18,19]. This approach resulted in the classification accuracies ranged between 78 to 95% depending on the category. The two events *stable keyhole* and *unstable keyhole* could be classified with 89 and 84% confidence. The capability to distinguish those two events is very promising for in situ and real time quality control since *unstable keyhole* often leads to defects.

The potential of this approach has also been demonstrated for in situ quality control of additive manufacturing by Wasmer et al. [8] and Shevchik et al. [11]. These results show that the combination of the wavelet decomposition and machine learning is a promising solution for in situ and real-time control of the process using AE and optical sensors. Due to the simplicity of the hardware setup, the control unit can be easily realized in industrial sector.

4. Conclusion

In situ and real-time quality control of laser welding is still a challenge today. The reason is the highly complex and dynamical laser material-interaction. To address this, in this contribution, we combined AE and optical sensing techniques to study the laser welding process of aluminum. To overcome the difficulties of post mortem correlation between the recorded signals with the different momentary events, the experiments were conducted with a high-speed X-ray imaging. The results showed that both AE and optical sensors were complimentary to each other in detecting different regimes of the process including surface melting, keyhole and resolidification. The events that could lead to defect formation, however, could not be sufficiently recognized by human visual inspection of the signals. Actually, it is due to the complex dynamic and short time spans of the events, such as keyhole fluctuation, pore formation and spattering. Therefore, the correlation between the signals and the post mortem quality analysis is not reliable. The combination of advances in signal processing and state-of-the-art statistical techniques such as wavelet decomposition and machine learning is a promising approach for quality control of laser welding based on AE and optical sensors.

Acknowledgements

We would like to thanks Dr. Jörg Grenzer from Helmholtz-Zentrum Dresden-Rossendorf and Dr. Christian Leinenbach from Empa for the X-ray support during the beam time. Beamtime was granted by the European Synchrotron Radiation Facility (MA-3477).

References

- [1] Maiman TH. Stimulated Optical Radiation in Ruby. *Nature* 1960;187:493–4. doi:10.1038/187493a0.
- [2] Courtois M, Carin M, Le Masson P, Gaied S, Balabane M. A complete model of keyhole and melt pool dynamics to analyze instabilities and collapse during laser welding. *J Laser Appl* 2014;26:42001. doi:10.2351/1.4886835.
- [3] Fabbro R. Melt pool and keyhole behaviour analysis for deep penetration laser welding. *J Phys D Appl Phys* 2010;43:445501. doi:10.1088/0022-3727/43/44/445501.
- [4] Brock C, Tenner F, Klämpfl F, Hohenstein R, Schmidt M. Detection of Weld Defects by High Speed Imaging of the Vapor Plume. *Phys Procedia* 2013;41:539–43. doi:10.1016/j.phpro.2013.03.113.
- [5] Zhao H, Qi H. Vision-based keyhole detection in laser full penetration welding process. *J Laser Appl* 2016;28:22412. doi:10.2351/1.4944003.
- [6] Dupriez ND, Truckenbrodt C. OCT for Efficient High Quality Laser Welding. *Laser Tech J* 2016;13:37–41. doi:10.1002/latj.201600020.
- [7] Grosse C, Ohtsu M, editors. *Acoustic Emission Testing Basics for Research - Applications in Civil Engineering*. 1st ed. Springer, Berlin, Heidelberg; 2008. doi:10.1007/978-3-540-69972-9.
- [8] Wasmer K, Kenel C, Leinenbach C, Shevchik SA. In Situ and Real-Time Monitoring of Powder-Bed AM by Combining Acoustic Emission and Artificial Intelligence. In: Meboldt M, Klahn C, editors. *Ind. Addit. Manuf. - Proc. Addit. Manuf. Prod. Appl. - AMPA2017*. AMPA, Cham: Springer International Publishing; 2017, p. 200–9. doi:10.1007/978-3-319-66866-6_20.
- [9] Cocota JAN, Garcia GC, da Costa AR, de Lima MSF, Rocha FAS, Freitas GM. Discontinuity Detection in the Shield Metal Arc Welding Process. *Sensors (Basel)* 2017;17:1082. doi:10.3390/s17051082.
- [10] Vakili-Farahani F, Lungershausen J, Wasmer K. Wavelet analysis of light emission signals in laser beam welding. *J Laser Appl* 2017;29:22424. doi:10.2351/1.4983507.
- [11] Shevchik SA, Kenel C, Leinenbach C, Wasmer K. Acoustic emission for in situ quality monitoring in additive manufacturing using spectral convolutional neural networks. *Addit Manuf* 2017. doi:10.1016/j.addma.2017.11.012.
- [12] Olbinado MP, Just X, Gelet J-L, Lhuissier P, Scheel M, Vagovic P, et al. MHz frame rate hard X-ray phase-contrast imaging using synchrotron radiation. *Opt Express* 2017;25:13857–71. doi:10.1364/OE.25.013857.
- [13] Yilbas BSY and KD and Z. Measurement of temperature-dependent reflectivity of Cu and Al in the range 30-1000 degrees C. *Meas Sci Technol* 1991;2:668.
- [14] Berger P, Hügel H, Graf T. Understanding Pore Formation in Laser Beam Welding. *Phys Procedia* 2011;12:241–7. doi:10.1016/j.phpro.2011.03.031.
- [15] Mallat S, Hwang WL. Singularity detection and processing with wavelets. *IEEE Trans Inf Theory* 1992;38:617–43. doi:10.1109/18.119727.
- [16] Wasmer K, Le Quang T, Meylan B, Olbinado M, Rack A, Shevchik SA. Laser Processing Quality Monitoring by Combining Acoustic Emission and Machine Learning: A High-Speed X-Ray Imaging Approach. *Procedia CIRP*, 2018. doi:xx:xxx-xxx.
- [17] Mallat S. *A Wavelet Tour of Signal Processing*. Academic Press; 2009.
- [18] Friedman JH. Stochastic Gradient Boosting. *Comput Stat Data Anal* 2002;38:367–78. doi:10.1016/S0167-9473(01)00065-2.
- [19] Hastie T, Tibshirani R, Friedman J. *The Elements of Statistical Learning*. Springer-Verlag New York; 2009.